Solar Energy Materials & Solar Cells 117 (2013) 54–58

Contents lists available at ScienceDirect

Solar Energy Materials & Solar Cells

journal homepage: www.elsevier.com/locate/solmat

Nitride-based concentrator solar cells grown on Si substrates

C.Y. Liu [a], C.C. Lai [b], J.H. Liao [b], L.C. Cheng [c], H.H. Liu [c], C.C. Chang [a], G.Y. Lee [c], J.-I. Chyi [c], L.K. Yeh [d], J.H. He [d], T.Y. Chung [b], L.C. Huang [b], K.Y. Lai [b,*]

[a] Department of Chemical and Materials Engineering, National Central University, Chung-Li 320, Taiwan
[b] Department of Optics and Photonics, National Central University, Chung-Li 320, Taiwan
[c] Department of Electrical Engineering, National Central University, Chung-Li 320, Taiwan
[d] Institute of Photonics and Optoelectronics, National Taiwan University, Taipei 106, Taiwan

ARTICLE INFO

Article history:
Received 25 January 2013
Received in revised form
6 May 2013
Accepted 7 May 2013
Available online 6 June 2013

Keywords:
InGaN
GaN
Si substrates
Concentrator

ABSTRACT

InGaN/GaN multiple-quantum-well solar cells were grown on (111) Si substrates. AlN/AlGaN superlattice and self-assembly Si_xN_y masking islands were employed to alleviate the material mismatches between Si and GaN. The devices were characterized under the illumination of AM 1.5 G with different solar concentrations. As the concentration ratios increased from 1-sun to 105-sun, energy conversion efficiency was enhanced by 25%, which was noticeably greater than the enhancement reported on sapphire substrates under similar solar concentrations. The result is attributed to the superior heat sinking of Si substrates.

1. Introduction

The commercial success of blue/green LEDs, followed by the promising market of blue/green laser diodes and power electronics, has made GaN one of the most important semiconductors in the post-Si age. In 2002, the band gap of InN was found to be around 0.7 eV [1], rather than the previously claimed 1.9 eV [2]. The discovery signals an additional application for III-nitrides: photovoltaic devices, which is due to the potential for nearly full solar spectrum absorption. Not only promising for broadband absorption, nitride alloys also exhibit many other favorable photovoltaic properties, such as superior radiation resistance [3], large absorption coefficients [4], high saturation velocities [4], etc. All of these merits have attracted much research interest in nitride solar cells during the last decade.

Converting nitrides' photovoltaic potential into success hinges on the quality-price ratio. That is to say, in the pursuit of device performances, the efforts into nitride solar cells should also be investigated on cost reduction. One way to achieve the goal is to replace the substrate. In this regard, Si has been an attractive alternative to sapphire, which is currently the most-used substrate for nitride-based devices. Being the second abundant element in the earth's crust and the prime material in the well-developed IC industry, Si is always among the targets to be integrated for various devices made of compound semiconductors. Moreover, Si holds another advantage of cooling capability comparing to sapphire. The 4-fold larger thermal conductivity of Si (C_{si}=142 W/m k [5] vs. $C_{sapphire}$=36 W/m k [6]) promises much faster thermal dissipation, which is strongly desired for the devices under high-temperature operations. Seeing the potential in cost reduction and cooling ability, many research groups have devoted efforts to GaN-on-Si technologies [7–9]. But most of the focuses are on LEDs, the reports on solar cells are scarcely found.

The other approach to reducing the cost of nitride solar cells is to concentrate solar intensities. A concentrator solar cell collects large areas of sunlight via focusing lens or sun-tracking mirrors. By doing this, the electrical power generated by a unit cell area can be considerably enhanced, hence the cost on cell material is saved. Solar cells employing concentrator systems currently hold the record efficiency of 43.5% [10] and are projected to deliver the lowest \$/W ratio [11]. Concentrator cells, usually operating at extremely high temperatures, are particularly attractive to the material system of GaN-on-Si in light of its thermal dissipation advantage over sapphire. Yet, no research results on this topic are published to date.

In this study, we demonstrate the first nitride-based concentrator solar cells grown on Si substrates. Upon the increase in solar concentrations, photovoltaic performances of the solar cells are dramatically improved. Specifically, energy conversion efficiency (η) under the illumination of 105 suns is enhanced by 25%, which is in excess of those achieved on sapphire substrates under similar concentration ratios. Detailed analyses of the distinct photovoltaic behaviors from those on sapphire will be presented.

* Corresponding author. Tel.: +886 3 4227151x25256; fax: +886 34252897.
E-mail address: kylai@ncu.edu.tw (K.Y. Lai).

0927-0248/$ - see front matter
http://dx.doi.org/10.1016/j.solmat.2013.05.017

2. Experiment

The solar cells were grown by metal–organic chemical vapor deposition on (111) Si substrates. In order to accommodate the lattice mismatch between GaN and Si, AlN/AlGaN superlattices were used as the buffer layer to release the tensile stress in GaN [12]. Between each period of AlN/AlGaN, a Si_xN_y masking layer is inserted in an attempt to block the undesired threading dislocations propagating toward the active region. The dislocation-blocking layer is achieved through the reaction between ammonia and silane, from which Si_xN_y islands are self-assembled on the surface. These Si_xN_y islands have been shown effective in bending the dislocations horizontally and facilitating the coalescence of GaN islands with a great reduction in defect densities [13]. The thickness of the entire superlattice region is approximately 1.5 μm. Following the superlattice, the device structure consists of a 6-pair InGaN(2.5 nm)/GaN(14 nm) multiple quantum wells (MQW) sandwiched by a 0.6-μm n-type GaN (n-GaN) and a 70-nm p-type GaN (p-GaN). The MQW structure is adopted with two purposes: (i) to avoid crystal deterioration of the InGaN layers exceeding the critical thickness on GaN [14] and (ii) to gain an additional freedom in manipulating the open-circuit voltage (V_{oc}) through the band gaps of barrier layers [15]. V/III ratios of the MQW structure are 6850 for the wells and 9515 for the barrier, rendering the photoluminescence (PL) peak at 460 nm. Substrate temperatures for the AlN/AlGaN superlattice, n-GaN and p-GaN, the MQW were 720 °C, 1120 °C and 860 °C, respectively.

Device fabrication was carried out with standard procedures. Photolithography was used to define the $1 \times 1\ \mathrm{mm}^2$ mesa area. Inductively coupled plasma etching was then used to expose the n-GaN area. The transparent contact layer on p-GaN was made by Ni(5 nm)/Au(5 nm) deposited with the e-beam evaporation system, followed by an annealing process at 500 °C in air for 20 min. Finally, the layers of Cr(5 nm)/Au(300 nm) were deposited on p-GaN and n-GaN to form the electrodes.

3. Results and discussion

Fig. 1 presents the ω-2θ scan x-ray diffraction (XRD) around the (002) reflection of the MQW solar cell. The figure clearly delineates the InGaN satellite peaks as well as the peaks from AlN/AlGaN superlattice. Since the distance between adjacent satellite peaks is determined by the thickness of one QW period [16], the defined InGaN peak positions indicate abrupt interfaces between the wells and the barriers. The indium composition of the MQW can be estimated with the method proposed by Tsuda et al., where the InGaN layers are assumed to grow coherently on the underlying GaN layer and free to expand in the growth direction when being compressed by the in-plane strain [17]. In this case, the stress along the growth direction vanishes. Details of the estimation can be found in Refs. [17,18]. The indium composition obtained with this approach is around 15.2%.

Fig. 2 shows the external quantum efficiencies (EQE) of the MQW solar cell. The measurement was carried out under monochromatic illumination with a halogen lamp coupled to a monochromator. The efficiencies are maximized at the wavelength of 360 nm, which is much shorter than the PL peak wavelength at 460 nm. The blue-shift of EQE spectra can be attributed to the distinct mechanisms in the processes of photon emission and absorption. In emission, electrons generally relax to the lowest energy states in conduction band before being recombined with holes, whereas in absorption the carriers can be pumped to higher states as long as the absorbed photon energy is sufficient to trigger the carrier excitation. In addition, it is noticed that the EQE envelope is not symmetric about the peak wavelength. The result implies non-uniform distribution of indium contents in the active region, which can be caused by the low miscibility of InN in GaN [19]. Similar observations have been reported in our previous studies [20,21].

Photovoltaic properties of the solar cells on the Si substrate are revealed in Fig. 3(a), where the *J–V* curves were characterized under the illumination of solar simulator AM 1.5 G with the concentration ratios up to 105 suns. The measured device performances are summarized in Table 1. One can see that J_{sc}'s and η's presented here are lower than those reported on sapphire substrates [20–23], which is not surprising considering the infancy of the growth/fabrication conditions on Si. The high densities of threading dislocations in the epitaxial layers, stemming from the large mismatches between GaN and Si in lattice constant (17%) and thermal expansion coefficient (54%), are generally regarded as the culprit for the efficiency loss of nitride devices built on Si [8,12,13]. In particular, the huge thermal mismatch, being much larger than that (34%) between GaN and sapphire, often induces wafer cracks during temperature ramping when the layer thickness on Si reaches a certain extent. Therefore, the epitaxial thickness of GaN on Si is generally below 2 μm [12,13], while that of GaN on sapphire can easily exceed 4 μm [22,23]. It should be noted that the density of threading dislocations can be effectively reduced by

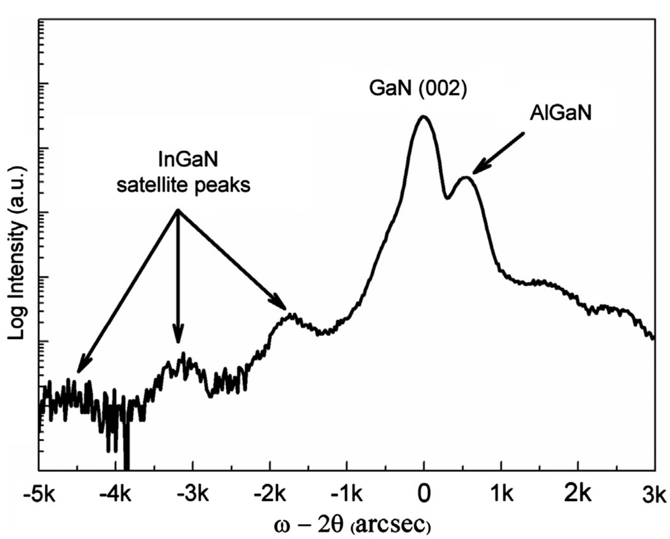

Fig. 1. XRD ω-2θ scan of the InGaN/GaN MQW solar cell grown on the Si substrate.

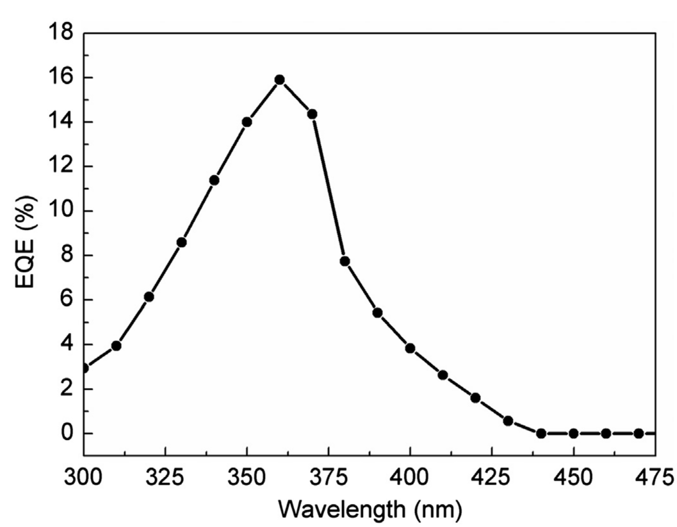

Fig. 2. EQE spectra of the MQW solar cell on the Si substrate.

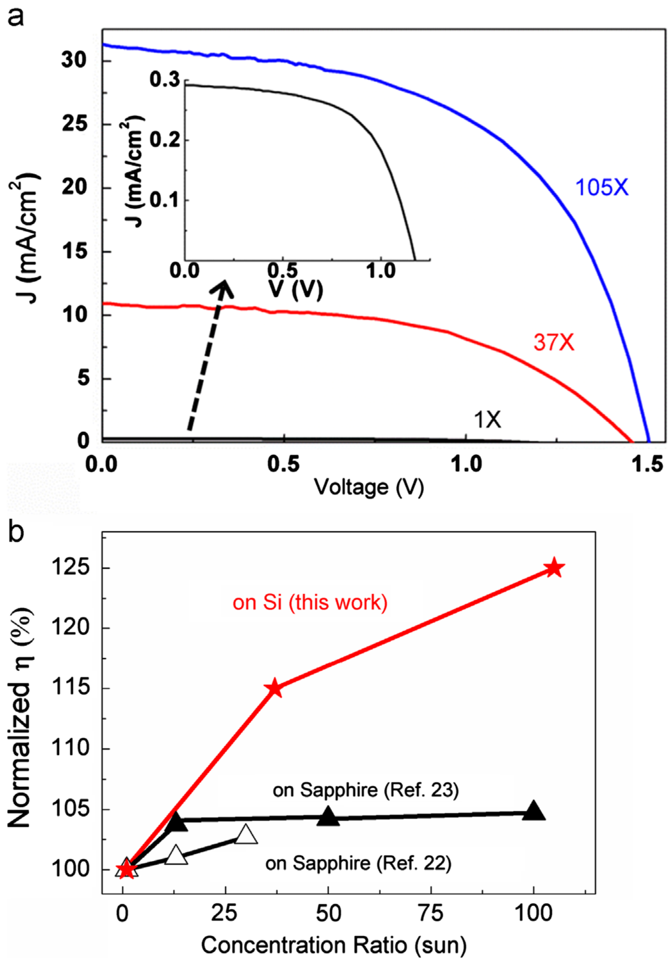

Fig. 3. (a) *J–V* curves of the MQW solar cell on the Si substrate measured under AM 1.5 G with different solar concentrations. (b) Normalized conversion efficiencies (η) as a function of solar concentrations on Si and on sapphire. The absolute values of η at 1-sun on Si, Sapphire (Ref. [22]) and Sapphire (Ref. [23]) are 0.20%, 2.95% and 2.13%, respectively.

Table 1
Device characteristics of the MQW solar cell on the Si substrate measured under AM 1.5 G with different solar concentrations.

Solar concentration	J_{sc} (mA/cm^2)	V_{oc} (V)	FF (%)	η (%)	Ideality factor
1-sun	0.29	1.17	60	0.2	4.2
37-sun	11.13	1.46	52	0.23	1.9
105-sun	31.32	1.51	56	0.25	1.3

increasing layer thickness, as threading dislocations tend to bend or combine with one another when propagating from the GaN/substrate interface, leading to the improved lattice quality in the region further away from the substrate [24]. In other words, the limited growth thickness should be an important factor to the inferior crystal qualities of GaN on Si. In addition to the AlN/AlGaN superlattice and Si_xN_y islands, material improvement can be made through the nanoheteroepitaxy technique, in which the contact area of heteroepitaxy is reduced to nanoscale and thus the occurrence of crystal defects is deferred by laterally releasing the lattice strain. GaN grown with nanoheteroepitaxy has been reported to exhibit superior crystal qualities [9]. For the active region, the well/barrier widths also need further optimization to enhance the photovoltaic performances on Si. An ideal well/barrier combination should be the one with sufficient optical absorption in the wells while rendering efficient carrier collection by the tunneling effect through the barriers. In device fabrication, the photocurrents can be increased by the so-called thin-GaN process, where the device structure is firstly bonded to a new substrate and the original Si substrate is removed by wet etching. The fabrication process is in analogy with the inverted metamorphic approach, which is commonly used in III–V multijunction solar cells [25]. The nitride solar cell built with thin-GaN process can be furnished with the micro-roughened surface and the back reflector [26], both of which can enhance the optical absorption by the MQW. The technologies of nanoheteroepitaxy and thin-GaN fabrication are currently under development in order to improve the conversion efficiencies.

Although the device performances are still in the process of optimization, Fig. 3(a) reveals some promising trait of the solar cells fabricated with GaN-on-Si. It is found that the efficiency of the MQW solar cell is noticeably enhanced under concentrated solar intensities. Increasing solar concentration from 1 sun to 105 suns respectively boosts J_{sc} and V_{oc} by 108-fold and 1.29-fold, resulting in the enhancement of η by 25%. The enhancement of photovoltaic performances on Si is significantly greater than those on sapphire under similar solar concentrations, according to the results previously reported by two other groups [22,23]. The distinct trends on the two types of substrates become apparent when η is normalized to the value under 1-sun illumination and plotted as a function of concentration ratios, as shown in Fig. 3(b). It can be seen that the improvement of η on sapphire is still less than 5% at 100 suns [23], while that on Si rapidly goes beyond 15% once the concentration ratio passes 37 suns. When the solar illumination is intensified, the larger J_{sc} is due to the increased number of electrons excited from the valence band, and the larger V_{oc} comes from the logarithmic dependence on J_{sc}:

$$V_{oc} = \frac{nkT}{q} \ln\left(\frac{J_{sc}}{J_o} + 1\right) \quad (1)$$

where n, k, T, q and J_0 are the ideality factor, Boltzmann constant, temperature, electronic charge and the diode saturation current density, respectively. It should be noted that the improvement brought by high solar concentrations is always accompanied by the side effect of junction heating, which in general degrades the photovoltaic performances via the shrinkage of V_{oc} and fill factor (FF) [22,23,27]. The increased V_{oc} at 105-sun condition indicates that the enhancement contributed by J_{sc} outweighs the negative effects induced by junction heating.

The results seen in Fig. 3(b) are believed to root in the different thermal conductivities of the substrates. The relative large thermal conductivity of the Si substrate provides efficient heat spreading at multi-sun conditions, preventing the significant climbing of J_0 and hence maintaining the increase in V_{oc} due to the increased photocarriers. A detailed explanation can be given as follows: the relatively poor performances at 1-sun condition are mainly caused by the high parasitic current loss because of the leakage through the device perimeter. The peripheral current leakage is particularly severe in our devices considering the small surface area of 1 mm^2, which leads to a very high perimeter area (perimeter × mesa thickness) to active area ratio. The severe leakage accounts for the large ideality factor at 1 sun shown in Table 1, which is extracted from Eq. (1) with J_0 determined from the dark current and the substrate temperature estimated with the numerical method to be described later. The undesired parasitic loss should be mitigated at high solar concentrations. This is because the significantly intensified carrier generation in the MQW is expected to induce Auger recombination in the bulk region, which makes the parasitic effect less influential and may reduce the leakage currents [28]. The mitigated parasitic loss resonates with the decreased ideality factors in concentrated conditions (Table 1), indicating the photocurrents are not only

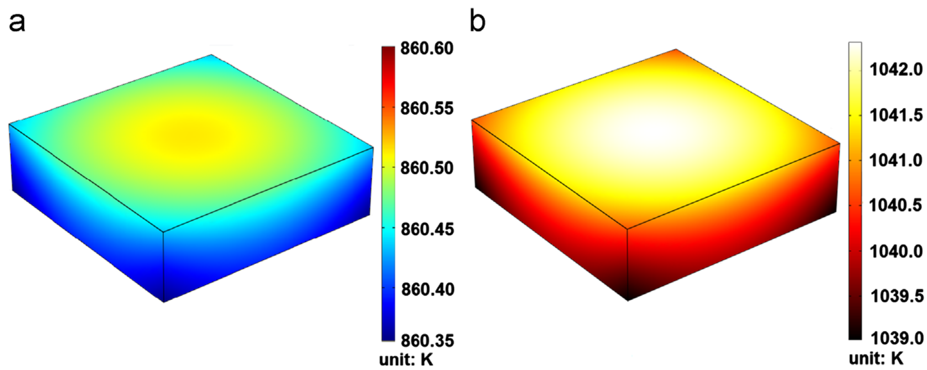

Fig. 4. Temperature distribution under the illumination of 105-sun AM 1.5 G spectrum for (a) the Si substrate and (b) the sapphire substrate. Substrate dimension: $1 \times 1 \times 0.37$ mm^3.

multiplied by the intensified irradiance but also collected by the electrodes with improved efficiencies. Similar observations of decreased current leakage were also observed with Si and GaAs concentrator solar cells [29,30].

On the other hand, the enhanced photovoltaic performances at high concentrations should simultaneously experience a counter-balancing influence exerted by the heating effect. The heating effect in concentrator solar cells can be enormous. The estimation of the substrate temperatures at different concentration ratios can be made using commercial software (Comsol Multiphysics, version 3.5) with a built-in Heat Transfer Module. In the calculation, the heat delivered to the substrate is governed by Stefan–Boltzmann law: $P = \rho T^4$, where P is the emission power and $\rho = 5.67 \times 10^{-8}$ W/m^2 K^4 is the Stefan–Boltzmann constant. Under the illumination of solar irradiance, thermal equilibrium in the substrate is reached through free convection and radiation to the air. Fig. 4 (a) and (b) respectively show the temperature distribution in the Si substrate ($C_{\mathrm{si}} = 142$ W/m k; emissivity = 0.60) and the sapphire substrate ($C_{\mathrm{sapphire}} = 36$ W/m k; emissivity = 0.25) [5,6,31,32] at 105 suns. The results are obtained by setting the optical absorption efficiency of 80%, and the substrate dimension of $1 \times 1 \times 0.37$ mm^3. One can see that the temperature in Si is much lower than that in sapphire. The highest surface temperature on Si is around 860.5 K, while that on sapphire is as high as 1042.3 K. The superior heat dissipation of Si is also manifested by the observation that the maximum temperature difference in the Si substrate is less than 0.2 K, while that in sapphire is close to 3 K.

The substantially higher temperature on sapphire degrades solar cell performances through the enlarged saturation current density J_0. The strong temperature dependence of J_0 is well known according to the relationship [33]:

$$J_0 = \frac{qD}{LN_D} n_i^2 = \frac{qD}{LN_D} BT^3 \exp\left(\frac{-E_{go}}{kT}\right) \quad (2)$$

where D and L are respectively the diffusivity and diffusion length of the minority carriers, N_D the doping, n_i the intrinsic carrier concentration, E_{g0} the band gap at 0 K and B is a temperature-independent constant. The exponential and third-power dependence of T makes J_0 dramatically increased as the concentration ratio rises. The increased J_0 not only brings down V_{oc} according to Eq. (1), but also lowers FF by reducing shunt resistance of the diode [34]. The decreased V_{oc} and FF contribute to the negative effect on η of the device. In comparison with the case on sapphire, it is believed that the superior cooling ability of the Si substrate delays heat accumulation in the active region, and therefore sustains the significant enhancement of η under concentrated irradiance. Combining the effects of leakage mitigation and thermal degradation, the InGaN MQW solar cells fabricated on Si substrates enjoy the advantage of fast heat dissipation over their counterparts on sapphire, making GaN-on-Si an attractive material system for concentrator solar cells.

4. Conclusions

InGaN/GaN MQW solar cells were grown on (111) Si substrates with strain-relieving AlN/AlGaN superlattice buffer layers. Well-defined InGaN satellite peaks revealed by ω-2θ XRD scan indicated clear well/barrier interfaces in the MQW. Under the illumination of 1-sun AM 1.5 G, the solar cell exhibited η of 0.2%. The modest performance was mainly due to crystal imperfections and peripheral current leakage. Photovoltaic performances of the MQW solar cell were improved at high solar concentrations. The improvement in η greatly exceeded those reported on sapphire substrates, and the results were attributed to the superior cooling capability of Si. Although the solar cell fabricated with GaN-on-Si still needs much more R&D to improve device performance, the research presented points out the promising potential of nitride-based photovoltaics for concentrator systems.

Acknowledgments

The research was supported by National Central University's Plan to Develop First-class Universities, Top-level Research Centers Grants 102G903-2, and National Science Council Grants NSC-102–3113-E-008-001 and NSC-100–2218-E-008–015.

References

[1] J. Wu, W. Walukiewicz, K.M. Yu, J.W. Ager III, E.E. Haller, Hai Lu, William J. Schaff, Yoshiki Saito, Yasushi Nanishi, Unusual properties of the fundamental band gap of InN, Applied Physics Letters 80 (2002) 3967–3969.
[2] T.L. Tansley, C.P. Foley, Optical band gap of indium nitride, Journal of Applied Physics 59 (1986) 3241–3244.
[3] J. Wu, W. Walukiewicz, K.M. Yu, W. Shan, J.W. Ager III, E.E. Haller, H. Lu W.J. Schaff, W.K. Metzger, S. Kurtz, Superior radiation resistance of $In_{1-x}Ga_xN$ alloys: full-solar-spectrum photovoltaic material system, Journal of Applied Physics 94 (2003) 6477–6482.
[4] Y. Nanishi, Y. Saito, T. Yamaguchi, RF-molecular beam epitaxy growth and properties of InN and related alloys, Japanese Journal of Applied Physics Part 142 (2003) 2549–2559.
[5] H.R. Shanks, P.D. Maycock, P.H. Sidles, G.C. Danielson, Thermal conductivity of silicon from 300 to 1400 °K, Physical Review 130 (1963) 1743–1748.
[6] C. Mion, Investigation of the Thermal Properties of Gallium nitride Using the Three Omega Technique, Ph.D. Dissertation, North Carolina State University, Raleigh, 2005.
[7] T. Egawa, B. Zhang, H. Ishikawa, High performance of InGaN LEDs on (1 1 1) silicon substrates grown by MOCVD, IEEE Electron Device Letters 26 (2005) 169–171.
[8] A. Dadgar, C. Hums, A. Diez, J. Blasing, A. Krost, Growth of blue GaN LED structures on 150-mm Si(1 1 1), Journal of Crystal Growth 297 (2006) 279–282.

[9] G.-T. Chen, J.-I. Chyi, C.-H. Chan, C.-H. Hou, C.-C. Chen, M.-N. Chang, Crack-free GaN grown on AlGaN/(1 1 1)Si micropillar array fabricated by polystyrene microsphere lithography, Applied Physics Letters 91 (2007) 261910-1–261910-3.
[10] Data Adopted from the Best Research-Cell Efficiencies Reported in 2012 by National Renewable Energy Laboratory (NREL), CO, USA. Results available at: 〈http://en.wikipedia.org/wiki/File:PVeff(rev120209).jpg〉.
[11] R.M. Swanson, The promise of concentrators, Progress in Photovoltaics: Research and Applications 8 (2000) 93–111.
[12] A. Dadgar, J. Christen, T. Riemann, S. Richter, J. Blasing, A. Diez, A. Krost, A. Alam, M. Heuken, Bright blue electroluminescence from an InGaN/GaN multi quantum-well diode on Si(1 1 1): impact of an AlGaN/GaN multilayer, Applied Physics Letters 78 (2001) 2211–2213.
[13] A. Krost, A. Dadgar, GaN-based devices on Si, Physica Status Solidi A 194 (2002) 361–375.
[14] P.M.F.J. Costa, R. Datta, M.J. Kappers, M.E. Vickers, C.J. Humphreys D.M. Graham, P. Dawson, M.J. Godfrey, E.J. Thrush, J.T. Mullins, Misfit dislocations in In-rich InGaN/GaN quantum well structures, Physica Status Solidi A 203 (2006) 1729–1732.
[15] K.W.J. Barnham, G. Duggan, A new approach to high-efficiency multi-band-gap solar cells, Journal of Applied Physics 67 (1990) 3490–3493.
[16] M.E. Vickers, M.J. Kappers, T.M. Smeeton, E.J. Trush, J.S. Barnard C.J. Humphreys, Determination of the indium content and layer thicknesses in InGaN/GaN quantum wells by x-ray scattering, Journal of Applied Physics 94 (2003) 1565–1574.
[17] M. Tsuda, H. Furukawa, A. Honshio, M. Iwaya, S. Kami-yama, H. Amano, I. Akasaki, Anisotropically biaxial strain in *a*-plane AlGaN on GaN grown on *r*-plane sapphire, Japanese Journal of Applied Physics 45 (2006) 2509–2513.
[18] K.Y. Lai, T. Paskova, V.D. Wheeler, T.Y. Chung, J.A. Grenko, M.A.L. Johnson, K. Udwary, E.A. Preble, K.R. Evans, Indium incorporation in InGaN/GaN quantum wells grown on *m*-plane GaN substrate and *c*-plane sapphire, Physica Status Solidi A 209 (2012) 559–564.
[19] I. Ho, G.B. Stringfellow, Solid phase immiscibility in GaInN, Applied Physics Letters 69 (1996) 2701–2703.
[20] K.Y. Lai, G.J. Lin, Y.-L. Lai, Y.F. Chen, J.H. He, Effect of indium fluctuation on the photovoltaic characteristics of InGaN/GaN multiple quantum well solar cells, Applied Physics Letters 96 (2010) 081103-1–081103-3.
[21] K.Y. Lai, G.J. Lin, C.-Y. Chen, Y.-L. Lai, J.H. He, Origin of hot carriers in InGaN-based quantum-well solar cells, IEEE Electron Device Letters 32 (2011) 179–181.
[22] R. Dahal, J. Li, K. Aryal, J.Y. Lin, H.X. Jiang, InGaN/GaN multiple quantum well concentrator solar cells, Applied Physics Letters 97 (2010) 073115.
[23] C.C. Yang, C.H. Jang, J.K. Sheu, M.L. Lee, S.J. Tu, F.W. Huang, Y.H. Yeh, W.C. Lai, Characteristics of InGaN-based concentrator solar cells operating under 150 × solar concentration, Optics Express 19 (2011) A695–A700.
[24] Yao Takafumi, Hong Soon-Ku (Eds.), Springer, Berlin, 2009.
[25] J.F. Geisz, Sarah Kurtz, M.W. Wanlass, J.S. Ward, A. Duda, D.J. Friedman J.M. Olson, W.E. McMahon, T.E. Moriarity, J.T. Kiehl, High-efficiency GaInP/GaAs/InGaAs triple-junction solar cells grown inverted with a metamorphic bottom junction, Applied Physics Letters 91 (2007) 023502.
[26] T. Fujii, Y. Gao, R. Sharma, E.L. Hu, S.P. DenBaars, S. Nakamura, Increase in the extraction efficiency of GaN-based light-emitting diodes via surface roughening, Applied Physics Letters 84 (2010) 855–857.
[27] M.J. Jeng, Y.L. Lee, L.B. Chang, Temperature dependences of $In_xGa_{1-x}N$ multiple quantum well solar cells, Journal of Physics D 42 (2009) 105101.
[28] R.A. Sinton, K. Young, J.Y. Gan, R.M. Swanson, 27.5-percent silicon concentrator solar cells, IEEE Electron Device LettersEDL-7 (1986) 567–569.
[29] R.A. Sinton, R.M. Swanson, Design criteria for Si point-contact concentrator solar cells, IEEE Transactions on Electron DevicesED-34 (1987) 2116–2123.
[30] H.F. MacMillan, H.C. Hamaker, N.R. Kaminar, M.S. Kuryla, M.L. Ristow, D.D. Liu, G.F. Virshup, J.M. Gee, 28% efficient GaAs concentrator solar cells, Photovoltaic Specialists Conference 1 (1988) 462–468.
[31] P.J. Timans, Emissivity of silicon at elevated temperatures, Journal of Applied Physics 74 (1993) 6353–6364.
[32] Data adopted from: 〈http://www.engineeringtoolbox.com/emissivity-coefficients-d_447.html〉.
[33] B.G. Streetman, Solid State Electronic Devices, Prentice-Hall, New Jersey, 1995.
[34] D.L. Pulfrey, On the fill factor of solar cells, Solid-State Electronics 21 (1978) 519–520.